J. Phys. B: At. Mol. Opt. Phys. **41** (2008) 215205 (7pp) doi:10.1088/0953-4075/41/21/215205

Electron collisions with sulfur compounds SO, SO_2 and SO_2AB (A, B = Cl, F): various total cross sections

K N Joshipura and Sumona Gangopadhyay

Department of Physics, Sardar Patel University, Vallabh Vidyanagar 388 120, India

E-mail: knjoshipura@yahoo.com

Received 26 June 2008, in final form 4 September 2008
Published 23 October 2008
Online at stacks.iop.org/JPhysB/41/215205

Abstract

This paper reports our theoretical investigations into electron scattering with SO, SO_2, SO_2Cl_2, SO_2ClF and SO_2F_2 in the energy range from the ionization threshold to 2000 eV. The present studies are prompted by the occurrence and applications of these molecular species in atmospheric and astrophysical systems, together with a paucity of data for SO and SO_2AB (A, B = Cl, F) species. Complex model potential calculations are carried out to find total elastic as well as inelastic cross sections, and ionization cross sections are retrieved from inelastic cross sections in a semi-empirical approximation. Comparisons with other data are made and discussed.

(Some figures in this article are in colour only in the electronic version)

1. Introduction

Total cross sections of electron impact on molecules like sulfur monoxide (SO), sulfur dioxide (SO_2), sulfuryl chloride SO_2Cl_2, sulfuryl chloride fluoride SO_2ClF and sulfuryl fluoride SO_2F_2 have important applications in space and atmospheric physics, plasma physics, environmental and atmospheric physics and astrophysics. Several forms of sulfur compounds are observed in interstellar clouds [1], although the reasons for the abundance of sulfur and sulfur-containing molecules are not clear. Electron collisions with sulfur compounds are induced in these systems by the interaction with solar flux of charge particles and also as a consequence of photoionization resulting in energetic secondary electrons.

The SO free radical is an abundant constituent of plasmas containing sulfur dioxide, SO_2. SO radicals are produced by electron-impact and ion-impact dissociation and by photodissociation of the parent SO_2 molecule [2–4]. There are various reasons for the ever-increasing interest in ionization processes in sulfur dioxide. Firstly, it is the most abundant pollutant of the Earth's atmosphere and secondly, as mentioned by Cadez *et al* [5] the presence of SO_2 has been proved in planetary atmospheres and interstellar clouds. SO_2 containing plasmas play an important role in planetary atmospheres such as the Jovian atmosphere and the plasma torus around Jupiter. Electron collisions on these molecules are also significant in its satellite Io. There are also applications related to diffuse-discharge switches to the plasma-assisted treatment of biocompatible materials [6]. Sulfuryl chloride (SO_2Cl_2) is a compound of industrial, environmental and scientific interest, see Szmytkowski *et al* [7]. Recently, SO_2Cl_2 has been suggested as the minor constituent of the Venus atmosphere where it might play a catalytic role. SO_2Cl_2 along with substituted compounds SO_2ClF and SO_2F_2 has a similar structure namely, tetrahedral and all three are polar molecules [7, 8]. Also included in our present study is a well-known polar molecule SO_2 for which experimental and theoretical studies have been reported by Orient *et al* [9] and Kim *et al* [10] respectively. In spite of the importance of these molecules, the information available on electron scattering for them is scarce.

Tarnovsky *et al* [2] have reported measurements for the absolute partial ionization cross sections for the formation of parent and fragment ions resulting from the electron-impact ionization and dissociative ionization of the SO free radical, from threshold to 200 eV. Except for these results, there are no other data available for SO to our knowledge, and hence the present study.

Compared to other targets of the present list, SO_2 is more intensively studied. There are numerous experimental

Table 1. Molecular properties[a] of SO, SO_2 and SO_2AB (A, B = Cl, F).

Target	First ionization potential I (eV)	Bond length (Å)	Polarizability (Å^3)	Dipole moment (au)
SO	10.29	S–O 1.481	–	0.610
SO_2	12.35	S–O 1.431	4.28	0.642
SO_2ClF	12.60	S–O 1.409 S–Cl 1.986 S–F 1.540	9.10	0.748
SO_2Cl_2	12.05	S–O 1.418 S–Cl 2.012	10.5	0.712
SO_2F_2	13.04	S–O 1.397 S–F 1.530	6.7	0.441

[a] See [7, 8, 14].

investigations compared to theoretical data. Szmytkowski and Maciag [11], Zecca *et al* [12] and Szmytkowski *et al* [13] have measured total (complete) cross sections while total ionization cross sections are given by Basner *et al* [6], Cadez *et al* [5], Orient *et al* [9] and Kim *et al* [10].

Recently, absolute total cross sections (TCS) for SO_2ClF have been measured by Szmytkowski *et al* [8] using linear transmission experiments at energies ranging from 0.6 to 370 eV. They [8] have also calculated total ionization and integral elastic cross sections using binary encounter Bethe (BEB) theory and independent atom model (IAM), respectively. Szmytkowski *et al* [7] have reported their measured total cross sections for SO_2Cl_2 from 0.5 to 150 eV, and calculated ionization and integral elastic cross sections for SO_2Cl_2 and SO_2F_2. However, they have not measured TCSs for SO_2F_2 but have added their elastic and ionization cross sections for total cross sections. Except for these results, no other experimental or theoretical data are available on sulfuryl halides.

We begin by defining the notations used for the various total cross sections in our present study. The total (complete) cross section of electron–molecule collisions is denoted by Q_T, and is the sum of the total elastic cross section Q_{el} and total inelastic cross section Q_{inel}. Thus

$$Q_T(E_i) = Q_{el}(E_i) + Q_{inel}(E_i). \quad (1)$$

Incident electron energy E_i in our case ranges from ionization threshold (∼10 eV) to 2000 eV. The quantity Q_{inel} is actually the cumulative total inelastic scattering cross section which is divided into two parts,

$$Q_{inel}(E_i) = \sum_n Q_{ion}(A^{+n}) + \Sigma Q_{exc}. \quad (2)$$

The first term in equation (2) accounts for the sum of all total ionization cross sections, for all energetically allowed states with A^{+n} as the charge state of the ion. The first term in equation (2) also includes dissociative ionizations of the target molecule. Therefore, our calculated Q_{ion} are actually compared with the sum total of single (both direct or parent plus dissociative) ionization together with double and higher ionizations of the target, as available in experimental data. The second term in equation (2) indicates the sum of total excitation cross sections for all allowed electronic transitions of the target by incident electrons.

Since the present targets are polar molecules, we have also determined the dipole rotational excitation cross section $Q_{rot}(\vec{D}, E_i)$ to represent non-spherical interactions. We, therefore, define the grand total cross section as

$$Q_{TOT}(E_i) = Q_T(E_i) + Q_{rot}(\vec{D}, E_i). \quad (3)$$

Here, $\vec{D}$ is the molecular dipole moment.

The present work aims at a comprehensive study by covering all major processes occurring in these targets, upon electron impact at intermediate and high energies. We have exhibited in table 1 the basic structural properties of our target molecules, employed in the present work.

2. Theoretical methodology

For the theoretical methodology adopted presently, we refer to our recent papers, see Joshipura *et al* [15–17], and omit details here. The e-molecule system is represented by a complex spherical potential, $V(r, E_i) = V_R(r, E_i) + iV_I(r, E_i)$, where r is the radial distance from the molecular centre of mass. The real part V_R of the complex potential includes the static potential, the exchange [18] and the polarization potentials. The spherically averaged molecular charge density $\rho(r)$, employed presently is determined from the constituent atomic charge densities derived from the wavefunctions of [19]. The polarization potential used here is of the form given by Zhang *et al* [20]. The imaginary term V_I of the complex potential, also called the absorption potential V_{abs} is adopted in a well-known non-empirical quasi-free model form given by Staszewska *et al* [21, see also [22, 23]]. Our modification in the original V_{abs} is discussed in [15–17]. The Schrödinger equation with the modified V_{abs} is solved by the variable phase approach [24], in order to determine Q_{el}, Q_{inel} and Q_T [25]. We denote by E_p the incident energy corresponding to the peak position of Q_{inel}.

Now, transitions to continuum leading to ionization correspond to infinitely many open channels, as against the electronic excitation, which comes mainly from a small number of discrete scattering channels. Therefore, ionization contribution in Q_{inel} increases as the incident energy increases above I, thereby making Q_{ion} dominate in $Q_{inel.}$. We can try to project out Q_{ion} from the known $Q_{inel.}$ in a reasonable approximation by starting with a ratio function,

$$R(E_i) = \frac{Q_{ion}(E_i)}{Q_{inel}(E_i)}. \quad (4)$$

In the complex scattering potential-*ionization contribution* (CSP-*ic*) method discussed in [15–17, 26], the ratio R is made target sensitive by expressing it as a function of a dimensionless variable $U = E_i/I$. Further as in [15–17, 26]

$$R(E_i) = 1 - C_1\left[\frac{C_2}{U+a} + \frac{\ln(U)}{U}\right]. \qquad (5)$$

Equation (5) involves the dimensionless parameters C_1, C_2 and 'a', which are determined by imposing three conditions on R (E_i) as in [15–17, 26]. Specifically, we have $0 \leqslant R \lesssim 1$, such that

$$R(E_i) = 0 \qquad \text{for} \quad E_i \leqslant I, \qquad (6a)$$

$$R(E_i) = R_p \qquad \text{for} \quad E_i = E_p \qquad (6b)$$

and

$$R(E_i) \cong 1 \qquad \text{for} \quad E_i > E_p. \qquad (6c)$$

Here, $R_p = 0.7$ stands for the value of the ratio R at $E_i = E_p$. The choice of this value is approximate but physically justified. The peak position E_p (typically around 50 eV or so) occurs at an incident energy where the discrete excitation cross sections in equation (2) are on the wane, while the ionization cross section is rising fast, suggesting that the R_p value should be above 0.5 but still below 1. We follow the general trend observed in wellknown well-known targets such as Ne, Ar, O_2, N_2, CH_4 [15–17, 26, 27], etc that near the peak value E_p, the contribution of the cross section Q_{ion} is about 70–80% in the total inelastic cross section Q_{inel} and the same increases with energy. This particular trend in the relative contributions of the two terms in equation (2) is explored in the CSP-*ic* method. However, the choice of R_p in equation (6) is not rigorous and it introduces uncertainty in the final results. For over two dozen atomic and molecular targets examined by us so far, the said uncertainty is found to be within the experimental errors ∼10–15% generally involved in ionization measurements. Therefore, it is worth trying to explore this method for the present targets.

We now turn briefly to the electron–molecule dipole potential, since all the present targets are polar molecules. Presently, we have adopted from Itikawa [28] a modification in the form of cut-off dipole potential (V_{DM}) defined below:

$$V_{DM} = -\frac{\vec{D}\cdot\hat{r}}{r_d^2} \qquad 0 \leqslant r \leqslant r_d$$

$$= -\frac{\vec{D}\cdot\hat{r}}{r^2} \qquad r > r_d, \qquad (7)$$

where $\vec{D}$ is the molecular dipole moment and r_d is chosen to be half of the shortest bond length in the target molecule. The above form is more justified than the asymptotic point-dipole potential $-\vec{D}\cdot\hat{r}/r^2$, which diverges at $r = 0$. The differential cross section for rotational excitation from the initial state of rotational quantum number J to the final state $J' = J \pm 1$ can be calculated analytically in the present dipole potential equation (7). The rotational cross section $Q_{rot}(E_i)$ is then obtained by numerical integration over scattering angle θ. The Q_{rot} thus calculated are added to the Q_T for obtaining the grand total cross sections Q_{TOT}, equation (3).

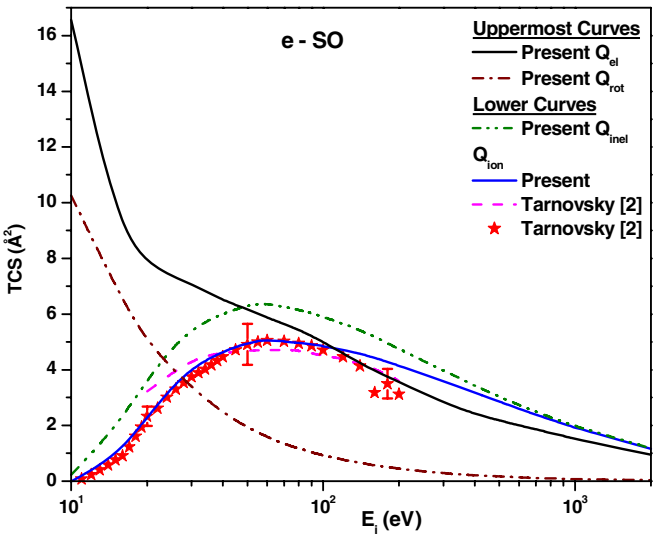

Figure 1. Electron scattering cross sections with SO. Uppermost curves: solid line–present Q_{el}; dash dot–present Q_{rot}. Lower curves: dash dot dot–present Q_{inel}; solid line—present Q_{ion}; dash line—Tarnovsky *et al* [2] Q_{ion}; star—Tarnovsky *et al* [2] Q_{ion}.

3. Results and discussion

The CSP-*ic* method defined through equations (4)–(6) has already been employed successfully to obtain total ionization cross sections of a number of atomic–molecular targets, as demonstrated in [15–17, 26]. The method though non-rigorous and semi-empirical is capable of delivering the important total cross sections of an electron–molecule system within acceptable accuracies. It is employed here to provide the major total cross sections Q_{TOT}, Q_T, Q_{el}, Q_{inel}, Q_{ion} and ΣQ_{exc} of electron scattering from SO, SO_2 and SO_2AB (A, B = Cl, F) at energies from threshold to 2000 eV. Let us first discuss our calculations for SO and SO_2 and then go over to the remaining lesser-known targets.

In figure 1, we have plotted total inelastic and total ionization cross sections for the SO radical and compared with the available results of Tarnovsky *et al* [2]. Very good agreement is observed between the measured values of Tarnovsky *et al* and the present Q_{ion} results from threshold to 100 eV, but above this the values of Tarnovsky *et al* [2] are lower than our values. The calculated total single ionization cross-sections [2] using the modified additivity rule for SO^+, shown by the dashed curve in figure 1, are lower beyond peak. The uncertainty in the determination of the absolute SO parent ionization cross section is about ±15% in [2]. The uppermost curve shows our present Q_{el}, followed by the dash-dot curve showing the Q_{rot} calculated by the cut-off dipole potential, equation (7). The present dipole cut-off model reduces the overestimation caused by the use of the first Born approximation. Our present cross sections are given in table 2.

In figure 2, we have made a comprehensive study of all major total cross sections for e-SO_2 scattering. Our present Q_T agrees well with Szmytkowski *et al* [11] and that of Zecca *et al* [12] from intermediate (∼30 eV) to high energy. At lower energies, our total cross sections are higher than that

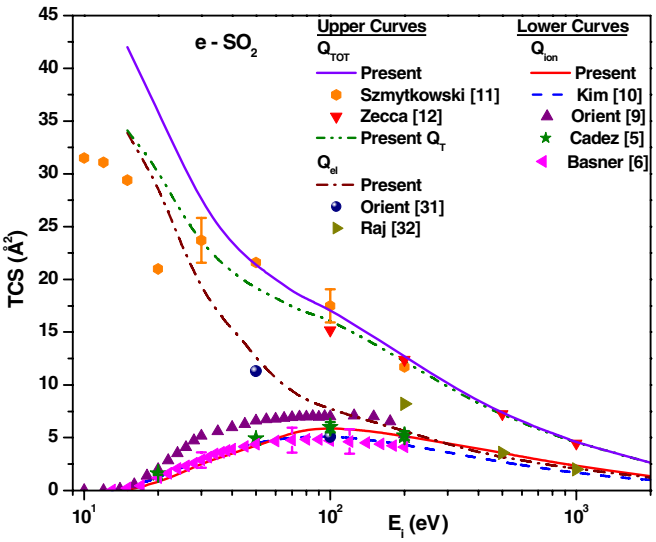

Figure 2. Electron scattering cross sections with SO_2. Upper curves: solid line—present Q_{TOT}; hexagon—Szmytkowski *et al* [11] Q_{TOT}; inverted triangle—Zecca *et al* [12] Q_{TOT}; dash dot dot—present Q_T; dash dot—present Q_{el}; sphere—Orient *et al* [29] Q_{el}; right triangle—Raj and Tomar [30] Q_{el}. Lower curves: solid line—present Q_{ion}; dash line—Kim *et al* [10]; triangle—Orient and Srivastava [9] Q_{ion}; star—Cadez *et al* [5] Q_{ion}; left triangle—Basner *et al* [6] Q_{ion}.

Table 2. Present Q_{el}, Q_{rot} and Q_{ion} (in Å^2) for SO.

	SO		
E_i (eV)	Q_{el}	Q_{rot}	Q_{ion}
10	16.57	10.26	0.23
15	9.37	6.98	0.88
20	7.72	4.94	2.28
30	7.09	3.36	4.02
40	6.49	2.45	4.64
50	6.18	1.93	4.95
60	5.87	1.58	5.06
70	5.64	1.33	5.02
80	5.44	1.18	4.97
90	5.21	1.03	4.91
100	5.00	0.92	4.85
150	4.08	0.60	4.51
200	3.56	0.44	4.15
300	2.82	0.28	3.60
400	2.41	0.21	3.18
500	2.18	0.17	2.86
600	2.00	0.14	2.60
700	1.86	0.11	2.39
800	1.73	0.10	2.21
900	1.62	0.09	2.06
1000	1.52	0.08	1.93
2000	0.95	0.04	1.16

of Szmytkowski *et al* [11]. We have compared our Q_{el} with Orient *et al* [29], and Raj and Tomar [30] and it agrees well at higher energies. The experimental elastic cross sections Q_{el} are obtained [29] by integrating the measured differential cross sections, so that the experimental Q_{el} involves a large error.

In order to account for anisotropic effects we have also calculated Q_{rot}, by the cut-off dipole and have plotted grand total cross section Q_{TOT} for SO_2 ($D = 0.642$ au). Towards

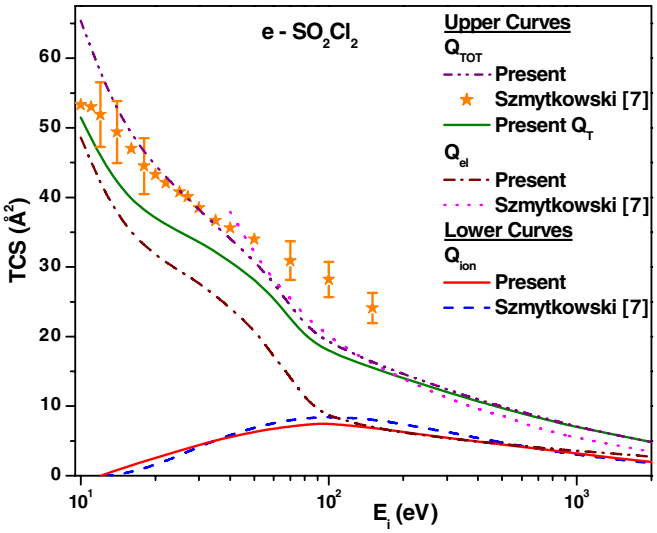

Figure 3. Electron scattering cross sections with SO_2Cl_2. Upper curves: dash dot dot—present Q_{TOT}; star—Szmytkowski *et al* [7] Q_{TOT}; solid line—present Q_T; dash dot—present Q_{el}; dot line—Szmytkowski *et al* [7] Q_{el}. Lower curves: solid line—present Q_{ion}; dash line Szmytkowski *et al* [7] Q_{ion}.

lower energies the measured Q_{TOT} are lower than the calculated results, and this behaviour is also observed in another polar molecule H_2O ($D = 0.728$ au), as mentioned in Itikawa and Mason [31].

The lower curves in figure 2 are of ionization cross sections. Large discrepancies exist between different experimental determinations of Q_{ion}. Our present Q_{ion} are compared with the BEB theory of Kim *et al* [10] and measured data of Orient and Srivastava [9], Cadez *et al* [5] and Basner *et al* [6]. The measurements of Cadez *et al* [5] are (15–30%) lower than those of Orient and Srivastava [9] but higher than that of Basner *et al* [6]. Our present Q_{ion} is well within the relative errors in cross section experiments of 8% as stated by Cadez *et al* [5]. The choice of 0.7 for R_P made in our calculations is semi-empirical. Therefore, we have also calculated Q_{ion} by letting R_p be 0.65 and 0.8 for the well-known target SO_2. The results with $R_p = 0.65$ are nearly the same as those with $R_p = 0.7$, which is more appropriate than 0.8. Therefore we continue with $R_p = 0.70$ unless stated otherwise. Our present Q_{TOT}, Q_T, Q_{el} and Q_{ion} for SO_2 are given in table 3.

Next in figure 3, we have plotted our various total cross sections for electron impact on SO_2Cl_2. Our results are compared with the only available data by Szmytkowski *et al* [7]. The authors [7] measured absolute total cross sections Q_{TOT} for electron scattering from SO_2Cl_2 molecules in a linear transmission experiment at energies 0.5–150 eV. Our present Q_T and Q_{el} are found to be lower than [7]. They [7] have calculated Q_{el} by the IAM and Q_{ion} by using BEB formalism, and hence have deduced their total cross sections Q_T as the sum of elastic and ionization cross sections. The authors [7] have stated that at intermediate energies, their own [7] experimental TCS results agree well with their own calculated total cross-section estimations.

Table 3. Present Q_{TOT}, Q_T, Q_{el} and Q_{ion} (in Å^2) for SO_2.

	SO_2					
E_i (eV)	Q_{TOT}	Q_T	Q_{el}	Q_{ion} $R_p = 0.65$	Q_{ion} $R_p = 0.7$	Q_{ion} $R_p = 0.80$
15	42.01	34.10	33.89	0.02	0.05	0.06
20	35.91	30.38	28.93	0.31	0.76	0.80
30	27.15	23.57	19.26	1.50	2.50	3.11
40	23.36	20.70	15.27	2.36	3.48	4.18
50	21.33	19.18	12.55	2.97	4.22	4.68
60	20.01	18.24	10.62	3.95	4.88	5.71
70	18.89	17.40	9.38	4.71	5.46	6.36
80	18.15	16.86	8.57	5.15	5.73	6.60
90	17.63	16.49	8.11	5.44	5.86	6.70
100	17.09	16.08	7.75	5.62	5.90	6.69
150	14.57	13.91	6.48	5.50	5.56	6.12
200	12.72	12.23	5.64	5.08	5.15	5.57
300	10.13	9.81	4.40	4.27	4.49	4.75
400	8.47	8.24	3.63	3.77	3.97	4.16
500	7.39	7.21	3.18	3.37	3.56	3.70
600	6.58	6.43	2.85	3.06	3.22	3.33
700	5.94	5.82	2.60	2.79	2.94	3.03
800	5.43	5.32	2.39	2.53	2.71	2.78
900	4.99	4.90	2.21	2.34	2.51	2.57
1000	4.55	4.55	2.06	2.16	2.34	2.39
2000	2.64	2.64	1.24	1.13	1.37	1.38

At 40 eV, the absolute grand total cross-section (Q_{TOT}) measured in [7] is 35.6 Å^2, and their calculated elastic cross section is 37.9 Å^2. This is not correct because Q_{el} being a part of Q_{TOT} we expect that at these energies, total elastic cross sections should be less than grand total cross section ($Q_{el} < Q_{TOT}$). This observation simply confirms the fact that the Q_{el} calculated [7] in the independent atom model with the static and polarization model potential are overestimating. The IAM disregards covalent bonding and other molecular properties, as it assumes each constituent atom of the molecule to scatter independently and thus the redistribution of the atomic electrons due to molecular binding is rendered unimportant. The estimated Q_{el} of [7] also ignores the dipolar nature of the target.

In order to account for anisotropic effects an approximate calculation is made in the present work to include dipole rotational total cross sections in the Born approximation. In order to check the overestimation of point dipole model we have considered presently our cut-off dipole potential V_{DM}, equation (7). At a close distance $r = r_d$, the incident electron is well within the target charge cloud and the asymptotic point-dipole potential is no longer valid. The cut-off model, equation (7), is more meaningful. The uppermost curve in figure 3 is our present Q_{TOT}, which provides a valid estimate of grand total cross section including all the major isotropic and anisotropic effects.

Considering next the ionization of SO_2Cl_2, our present Q_{ion} agrees well with the theoretically calculated ionization cross sections of Szmytkowski *et al* [7]. Their cross sections have been computed within the BEB formalism [10]. Our present total cross sections for SO_2Cl_2 are listed in table 4.

In figure 4, we have plotted all our total cross sections for the e–SO_2ClF system. The only available comparisons are the experimental data for absolute total cross sections (Q_{TOT})

Table 4. Present Q_{TOT}, Q_T, Q_{el} and Q_{ion} (in Å^2) for SO_2Cl_2.

	SO_2Cl_2			
E_i (eV)	Q_{TOT}	Q_T	Q_{el}	Q_{ion}
10	65.40	51.51	48.58	0.00
15	48.63	38.88	33.97	1.23
30	38.17	33.76	27.92	4.46
40	34.08	30.81	24.10	5.60
50	30.82	28.16	20.99	6.30
60	27.80	25.61	17.19	6.80
70	24.36	22.51	14.15	7.09
80	21.87	20.28	11.23	7.33
90	20.26	18.86	9.54	7.50
100	19.15	17.89	8.51	7.50
150	16.30	15.48	6.93	6.91
200	14.61	14.01	6.22	6.30
300	12.41	12.02	5.42	5.47
400	10.98	10.69	4.90	4.91
500	9.93	9.71	4.54	4.50
600	9.13	8.95	4.26	4.15
700	8.48	8.33	4.04	3.86
800	7.95	7.81	3.85	3.60
900	7.51	7.39	3.70	3.39
1000	7.02	7.02	3.57	3.19
2000	4.84	4.84	2.77	2.00

and the calculated elastic and ionization cross sections by Szmytkowski *et al* [8]. Both the experimental Q_{TOT} data and the elastic cross section Q_{el} of [8] are much higher than our present results in the intermediate energy range while lying low at lower energies. In this target too we have included the non-spherical contribution (Q_{rot}) and calculated Q_{TOT} for SO_2ClF.

Our present ionization cross sections for SO_2ClF agree well with Szmytkowski *et al* [8] till peak (90 eV) and are lower thereafter as compared to the cross sections calculated

Table 5. Present Q_{TOT}, Q_T, Q_{el} and Q_{ion} (in Å^2) for SO_2ClF_2 and SO_2F_2.

	SO_2ClF				SO_2F_2			
E_i (eV)	Q_{TOT}	Q_T	Q_{el}	Q_{ion}	Q_{TOT}	Q_T	Q_{el}	Q_{ion}
15	54.27	45.66	45.49	0.06	–	–	–	–
20	45.53	39.52	38.21	0.90	38.80	36.19	35.10	0.60
30	36.47	32.57	28.40	3.63	32.86	31.16	27.40	2.84
40	31.33	28.44	22.91	5.05	28.33	27.07	22.08	4.00
50	28.20	25.86	19.76	5.99	24.22	23.20	17.68	4.61
60	26.08	24.16	16.99	6.46	21.77	20.94	14.78	5.11
70	24.26	22.64	14.42	6.75	20.29	19.58	12.29	5.88
80	22.58	21.17	12.95	6.88	19.17	18.56	10.73	6.28
90	21.33	20.09	11.61	6.92	18.26	17.72	9.69	6.43
100	20.41	19.30	10.75	6.84	17.53	17.05	8.97	6.46
150	17.15	16.42	8.58	5.96	15.11	14.79	7.42	5.92
200	15.07	14.55	7.44	5.29	13.26	13.03	6.38	5.43
300	12.49	12.14	6.17	4.47	10.93	10.79	5.22	4.70
400	10.86	10.61	5.42	3.96	9.43	9.32	4.51	4.18
700	8.18	8.04	4.22	3.05	6.92	6.86	3.34	3.21
800	7.62	7.50	3.98	2.85	6.41	6.36	3.13	2.99
900	7.15	7.05	3.78	2.67	6.00	5.95	2.95	2.80
1000	6.66	6.66	3.61	2.52	5.61	5.61	2.81	2.63
2000	4.52	4.52	2.65	1.47	3.74	3.74	2.03	1.65

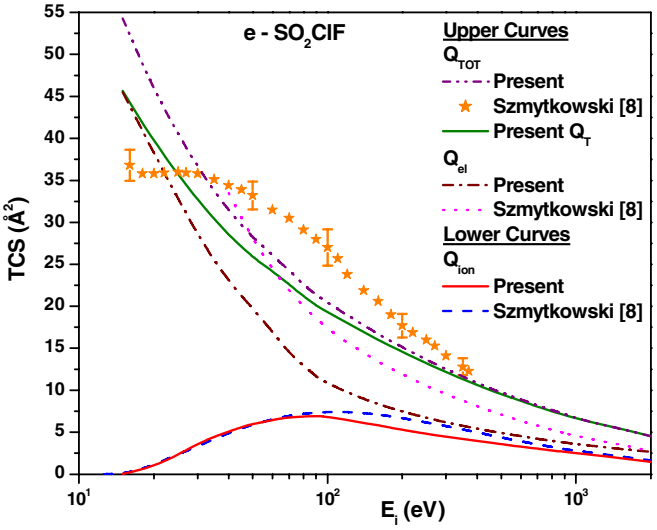

Figure 4. Electron scattering cross sections with SO_2ClF. Upper curves: dash dot dot—present Q_{TOT}; star—Szmytkowski *et al* [8] Q_{TOT}; solid line—present Q_T; dash dot—present Q_{el}; dot line—Szmytkowski *et al* [8] Q_{el}. Lower curves: solid line—present Q_{ion}; dash line Szmytkowski *et al* [8] Q_{ion}.

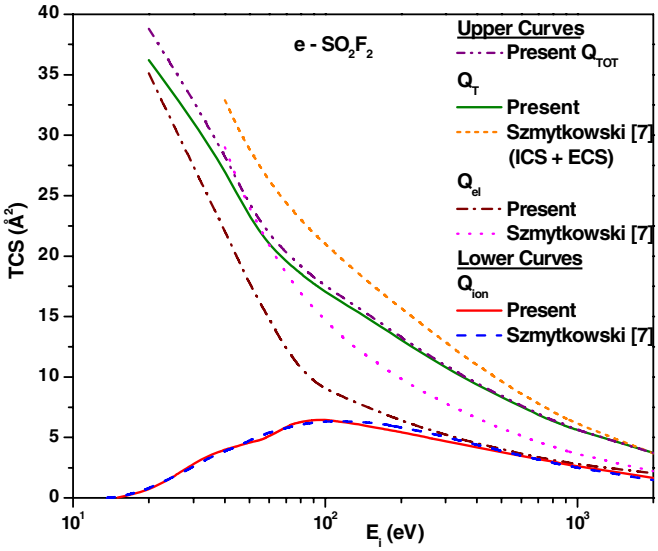

Figure 5. Electron scattering cross sections with SO_2F_2. Upper curves: dash dot dot—present Q_{TOT}; solid line—present Q_T; short dash—Szmytkowski *et al* [7] Q_T; dash dot—present Q_{el}; dot line—Szmytkowski *et al* [7] Q_{el}. Lower curves: solid line—present Q_{ion}; dash line—Szmytkowski *et al* [7] Q_{ion}.

[8] using the BEB formalism. Our present cross sections for SO_2ClF are exhibited in table 5.

Finally figure 5 shows all the present and earlier cross sections for electron impact on SO_2F_2. There are no experimental data available for this molecule. Szmytkowski *et al* [7] have calculated total cross sections as the sum of elastic and ionization cross sections in the energy range 40–4000 eV. Their ionization and elastic cross sections are calculated by using the BEB approximation and the IAM respectively. We have calculated Q_{TOT} for SO_2F_2, which includes Q_{rot} as done for SO_2Cl_2 and SO_2ClF. For SO_2F_2 Szmytkowski *et al* [7] have calculated total cross sections as the sum of ionization and elastic cross sections. The lower curves in figure 5 are ionization cross sections for SO_2F_2. Our present Q_{ion} agrees well with the ionization cross sections by Szmytkowski *et al* [7] calculated using the BEB formalism. The present Q_{TOT}, Q_T, Q_{el} and Q_{ion} are given in table 5.

In conclusion, the complex potential formalism along with the CSP-*ic* approximation enables us to obtain the total cross sections Q_T, Q_{el}, Q_{inel}, Q_{ion} and ΣQ_{exc}, while for polar molecules an approximate contribution of Q_{rot} can be included to determine the grand total cross section Q_{TOT}. It is thus possible to cover in our study almost all the important electron scattering processes occurring at intermediate and high incident energies. The work presented here offers an

extensive comparison with the previous data on a well-known target like SO_2. For systems like SO radical, together with SO_2AB (A, B = Cl, F) either isolated or no data have been reported previously. The present work will also be useful in terms of the new results reported herein.

Acknowledgments

This research forms a part of work being carried out under a project grant awarded to KNJ by the Indian Space Research Organization, Bangalore, India.

References

[1] Please see website www.oso.chalmers.se/centre/courses/exjobb-radioastronomi.html
[2] Tarnovski V, Levin A, Deutsch H and Becker K 1995 *J. Chem. Phys.* **102** 770
[3] Gatlinberti L 1988 *Pure Appl. Chem.* **60** 663
[4] Chang M B, Kushner M J and Rood M J 1992 *Plasma Chem. Plasma Proc* **12** 565
[5] Cadez I M, Pejcev V M and Kurepa M V 1983 *J. Phys. D: Appl. Phys.* **16** 305
[6] Basner R, Schmidt M, Deutsch H, Tarnovsky V, Levin A and Becker K 1995 *J. Chem. Phys* **103** 211
[7] Szmytkowski Cz, Mozejko P, Kwitnewski S, Domaracka A and Ptasinska-Denga E 2006 *J. Phys. B: At. Mol. Opt. Phys.* **39** 2571
[8] Szmytkowski Cz, Mozejko P, Kwitnewski S, Ptasinska-Denga E and Domaracka A 2005 *J. Phys. B: At. Mol. Opt. Phys.* **38** 2954
[9] Orient O J and Srivastava S K 1984 *J. Chem. Phys* **80** 140
[10] Kim Y-K, Hwang W, Weinberger N M, Ali M A and Rudd M E 1997 *J. Chem. Phys.* **106** 1026
[11] Szmytkowski Cz and Maciag K 1986 *Chem. Phys. Lett.* **124** 463
Szmytkowski Cz, Mozejko P and Kasperski G 1996 *XVIII Int. Symp. Phys. Ion Gases, Katar* 66
[12] Zecca A, Nogueira J C, Karwasz G P and Brusa R S 1995 *J. Phys B: At. Mol. Opt. Phys* **28** 477
[13] Szmytkowski Cz, Mozejko P and Krzysztofowicz A 2003 *Rad. Phys. Chem.* **68** 307
[14] Lide R 2005 *CRC Handbook of Chemistry and Physics* (Boca Raton, FL: CRC Press)
[15] Joshipura K N, Gangopadhyay S and Vaishnav Bhushit G 2007 *J. Phys. B: At. Mol. Opt. Phys* **40** 199
Joshipura K N, Vinodkumar M, Limbachiya C G and Antony B K 2004 *Phys. Rev.* A **69** 022705
[16] Joshipura K N, Vaishnav B G and Gangopadhyay S 2007 *Int. J. Mass Spectrom* **261** 146
[17] Joshipura K N, Gangopadhyay S, Limbachiya C G and Vinodkumar M 2007 *J. Phys. Conf. Series* **80** 012008
[18] Hara S 1967 *J. Phys. Soc. Japan* **22** 710
[19] Bunge C F and Barrientos J A 1993 *At. Data Nucl. Data Tables* **53** 113
[20] Zhang X Z, Sun J F and Liu Y F 1992 *J. Phys. B: At. Mol. Opt. Phys.* **25** 1893
[21] Staszewska G, Schwenke D M and Truhlar D G 1984 *J. Chem. Phys.* **81** 3078
[22] Fujimoto M M and Lee M T 2000 *J. Phys. B: At. Mol. Opt. Phys.* **33** 4759
[23] Blanco F and Garcia G 2003 *Phys. Rev.* A **67** 0022701
[24] Calogero F 1974 *Variable Phase Approach to Potential Scattering* (New York: Academic)
[25] Joachain C J 1984 *Quantum Collision Theory* (Amsterdam: North-Holland)
[26] Vinodkumar M, Limbachiya C, Korot K, Joshipura K N and Mason N 2008 *Int. J. Mass Spectrom.* **273** 145
[27] Karwasz G P, Brusa R S and Zecca A 2001 *Riv. Nuovo Cimento* **24** 1
[28] Itikawa Y 1978 *Phys. Rep.* **46** 117
[29] Orient O J, Iga I and Srivastava S K 1982 *J. Chem. Phys.* **77** 3523
[30] Raj D and Tomar S 1997 *J. Phys. B: At. Mol. Opt. Phys* **30** 1989
[31] Itikawa Y and Mason N J 2005 *J. Phys. Chem. Ref. Data* **34** 1